Understanding the Differing Fluid Phase Behavior of Cyclohexane + Benzene and their Hydroxylated or Aminated Forms

Y. Mauricio Muñoz-Muñoz[a], Chieh-Ming Hsieh[b] and Jadran Vrabec[a]*

[a]*Thermodynamics and Energy Technology, University of Paderborn, 33098 Paderborn, Germany*

[b]*Department of Chemical and Materials Engineering, National Central University of Taiwan, Jhongli, Taiwan*

Abstract

The three binary mixtures cyclohexane + benzene, cyclohexanol + phenol and cyclohexylamine + aniline exhibit qualitatively different vapor-liquid phase behavior, i.e. azeotropic with pressure maximum, azeotropic with pressure minimum and zeotropic, respectively. Employing molecular modeling and simulation, the COSMO-SAC model and a cubic equation of state, the root of these effects is studied on the basis of phase equilibria, excess properties for volume, enthalpy and Gibbs energy as well as microscopic structure. It is found that cyclohexane + benzene is characterized by more pronounced repulsive interactions, leading to pressure maximum azeotropy and a positive excess Gibbs energy. Functionalizing the aliphatic and aromatic rings with one amine group each introduces attractive hydrogen bonding interactions of moderate strength that counterbalance such that the mixture is zeotropic. The hydroxyl groups introduce strong hydrogen bonding interactions, leading to pressure minimum azeotropy and a negative excess Gibbs energy.

Keywords: cyclohexane, benzene, cyclohexanol, phenol, cyclohexylamine, aniline, vapor-liquid equilibria, molecular simulation, COSMO-SAC, cubic equation of state

*Corresponding author

E-mail address: jadran.vrabec@upb.de (J. Vrabec)

1. Introduction

The fluid phase behavior of the binary systems cyclohexane + benzene (mixture without functional groups), cyclohexanol + phenol (one hydroxyl group bonded to each of the rings) and cyclohexylamine + aniline (one amine group bonded to each of the rings) depends qualitatively on the functional group. Without a functional group, the binary mixture exhibits a pressure maximum azeotrope[1 2 3], with the hydroxyl group bonded to the rings, the binary system exhibits a pressure minimum azeotrope[4] and with the amine group bonded to the rings, the binary system is zeotropic[5]. The goal of this work was to elucidate the causes of this varying phase behavior.

The six considered cyclic hydrocarbons are also part of many industrial processes, e.g., in the food, pharmaceutical, paper, petrochemical, plastics, resins, rubber and textile industries, so that the present findings may contribute to technological aspects.

Benzene is a precursor of numerous products and is found in small amounts in crude oil. It can be produced by catalytic cracking or reforming, where the associated chemical reactions involve dehydrogenation of naphtenes or isomerization of alkylnaphtenes[6], while cyclohexane is obtained by catalytic hydrogenation of benzene in liquid or vapor phases[7]. Cyclohexane can be used as a hydrogen storage and transport medium or as a precursor of important chemical products. Efforts are continuing to catalyze the reverse hydrogenation reaction[8] and to yield cyclohexanol and cyclohexanone by electrocatalytic membrane reactors[9].

Cyclohexanol can be produced by oxidation of cyclohexane with hydrogen peroxide, tert-butyl hydroperoxide or molecular oxygen[10]. It can also be obtained by catalytic hydrogenation of phenol in the vapor phase, also yielding cyclohexanol and cyclohexanone[11]. As an innovative route, the direct hydration of cyclohexene by reactive distillation was recently proposed[12]. Phenol can be obtained by the Dow process or by the oxidation of cumene, in which a substantial amount of acetone is produced. In that process, chlorobenzene reacts at high temperature and pressure with an aqueous solution of sodium hydroxide to yield sodium phenoxide, which reacts with an acid to yield phenol[13]. This substance is used for various products, such as phenol-formaldehyde resins, which are constituted by phenol molecules linked by methylene groups. However, phenol is considered as an important environmental pollutant because it reduces the life expectancy of water ecosystems. Therefore, different methods for alleviating its environmental impact have been devised, e.g. heterogeneous photocatalysis[14] or pervaporation[15].

Amines, which are moderately polar substances and are present in a large variety of biological compounds, can be obtained by reductive amination, where ketones or aldehydes react with ammonia in the presence of a catalyst or sodium cyanotrihydridoborate. E.g., the reductive amination of cyclohexanone yields cyclohexylamine[13], which is produced by pressurized and catalyzed hydrogenation of aniline[16]. Cyclohexylamine is used in the rubber industry to delay the degradation of rubber mixtures and to prevent corrosion in steam power plants when it is added to water at concentrations of 5 ppm[17]. Aromatic amines, such as aniline or toluidine, can be produced by direct reduction of nitro compounds obtained from the nitration of aromatic compounds.

In this work, molecular modelling and simulation, the COSMO-SAC model[18] and a cubic equation of state (EOS) were applied to study the vapor-liquid phase behavior. Some studies on similar mixtures have been carried out in the past with the COSMO-SAC model, e.g. for the separation of the binary mixture cyclohexane + benzene employing ionic liquids[19] or liquid-liquid equilibria of the ternary mixture aniline + cyclohexylamine + water[20].

Molecular modeling and simulation is a versatile approach for studying both dynamic (e.g. diffusivity, viscosity, thermal conductivity) and static (e.g. phase equilibria, heat capacities, speed of sound) properties of fluids. It allows for elaborate interpretations of thermophysical properties from a microscopic point of view that are not possible with classical models, such as EOS. Simulation results are entirely determined by the underlying force fields, i.e. the mathematical representation of the molecular interactions[21]. These are nowadays developed on the basis of quantum chemical data and by optimization to experimental vapor-liquid equilibria (VLE)[22] or transport properties[23]. Some simulation studies have been carried out for phenol and aniline with rigid united-atom force fields[24 25] or with all-atom force fields with internal degrees of freedom[26] or by transfereable potentials for phase equilibria (TraPPE-EH)[27]. However, to the best our knowledge, only one of the three considered binary systems has been studied by molecular simulation, i.e. cyclohexane + benzene[26].

2. Methods and computational details

2.1. Force fields for cyclohexylamine, aniline and phenol

Simulations were carried out on the basis of force fields recently published by our group for cyclohexane[23], cyclohexanol[28] and benzene[29]. Models for phenol (C_6H_5OH), aniline ($C_6H_5NH_2$) and cyclohexylamine ($C_6H_{11}NH_2$) were developed in this work. The geometrical parameters of the rings were taken from the quantum chemical database provided by the National Institute of Standards and Technology (NIST)[30] in case of phenol, from a force field for benzene[29] in case of aniline and from a force field for cyclohexane[23] in case of cyclohexylamine. This also holds for the geometrical parameters of the hydroxyl and amine groups, i.e. the bond angles and the bond lengths between the atoms of the functional groups and the dihedral angles with respect to the rings[30]. In this way, the structure of all considered force fields is based on quantum chemical information. These properties between the functional groups and the rings were calculated with the *z* matrix[31]. Because the internal molecular degrees of freedom are of little importance for the present cyclic molecules, rigid molecular structures were assumed throughout.

The united atoms approach was applied to the rings such that the aromatic rings of phenol and aniline were represented by five identical methine LJ sites bonded to one carbon atom LJ site, which is carrying the hydroxyl or amine group. The aliphatic ring of cyclohexylamine was represented by five identical methanediyl LJ sites bonded to one methanetriyl LJ site, which is carrying the amine group.

The hydroxyl group was represented by one LJ site for the oxygen atom and one positive point charge for the hydrogen atom. A negative point charge was located in the center of the oxygen LJ site and to maintain electro-neutrality of the molecule, one positive charge was placed in the center of the carbon atom carrying the hydroxyl group. The amine group

was represented by one LJ site for the nitrogen atom and two positive point charges for the hydrogen atoms. In analogy to the hydroxyl group, a negative point charge was located in the center of the nitrogen LJ site and a positive charge was located in the center of methanetriyl group (cyclohexylamine) or carbon atom (aniline) carrying the amine group.

During the optimization procedure of the force fields, which is outlined in Figure 1, the LJ parameters of the methanetriyl site of cyclohexylamine, the carbon atom site of phenol and aniline and the LJ parameters of oxygen and nitrogen were kept constant. The LJ parameters for nitrogen and oxygen were taken from preceding work[32 33].

Initial values for the point charge magnitudes were taken from the NIST database[30]. Then, the optimization procedure shown in Figure 1 was carried out. Estimates for the saturated liquid density were obtained by isobaric-isothermal (NpT) ensemble simulations and proper VLE calculations were done with the grand equilibrium method[34]. Throughout, the *ms*2 code[35 36] was employed, wherein the intermolecular interactions are considered via the potential energy U

$$U = \sum_{i=1}^{N-1} \sum_{j=i+1}^{N} \left\{ \sum_{a=1}^{S_i^{LJ}} \sum_{b=1}^{S_j^{LJ}} 4\varepsilon_{ijab} \left[\left(\frac{\sigma_{ijab}}{r_{ijab}} \right)^{12} - \left(\frac{\sigma_{ijab}}{r_{ijab}} \right)^{6} \right] + \sum_{c=1}^{S_i^{e}} \sum_{d=1}^{S_j^{e}} \frac{1}{4\pi\epsilon_0} \frac{q_{ic} q_{jd}}{r_{ijcd}} \right\}, \quad (1)$$

where N is the number of molecules and S_i^{LJ} is the number of LJ sites of molecule i, i.e. S_i^{LJ}=7 for phenol, cyclohexylamine and aniline. r_{ijab} is the distance between the two LJ sites a and b, which belong to molecules i and j. S_i^e is the number of electrostatic charges of molecule i, r_{ijcd} is the distance between the charges c and d of magnitude q_{ic}, q_{jd}, which

belong to molecules i and j and ϵ_0 is the permittivity of vacuum. Figure 2 shows the force fields used in this work and Table 1 lists their parameters.

The VLE properties of all considered substances in their pure state are shown in Figures 3 to 6. The simulation results are compared with the DIPPR correlations[37] in case of cyclohexanol, phenol, cyclohexylamine and aniline as well as the reference equations of state for benzene[38] and cyclohexane[39]. Moreover, the available experimental literature data are shown.

Deviations between the present simulation results and the DIPPR correlations are shown in Figure 7. The absolute average deviations for phenol are 3.5% for vapor pressure, 0.3% for saturated liquid density and 5.6% for enthalpy of vaporization, considering the range where experimental data are available. The cyclohexylamine force field exhibits absolute average deviations of 4.7% for vapor pressure, 0.1% for saturated liquid density and 3.3% for enthalpy of vaporization. The absolute average deviations for aniline are 6.7% for vapor pressure, 0.4% for saturated liquid density and 7.2% for enthalpy of vaporization. The simulation results of the saturated vapor density are thermodynamically consistent [40]. To the best of our knowledge, experimental enthalpy of vaporization data are only available for cyclohexylamine[41] [42]. Thus, the deviation in terms of the enthalpy of vaporization for cyclohexylamine and phenol was calculated with derived data[43].

The critical points of the six considered pure fluids were calculated as well and they are shown in Figures 3-4 and Table 2. The critical temperature of phenol was slightly overestimated with respect to literature data[44], while critical pressure and density were underestimated with respect to literature data [44] [45]. The deviations are 1.0%, -5.6% and -

15.3%, respectively. Relative deviations of critical temperature, pressure and density with respect to literature data for cyclohexylamine[46] are -1.1%, -7.1% and 27%, respectively. Analogously, for aniline these numbers are -0.7%, -0.7% and -5.9%.

The second virial coefficient was predicted with the force field models considered in this work. These predictions were made for temperatures between 300 K and 1000 K by numerically integrating Mayer's f function. Figure 6 shows a comparison between the experimental virial coefficient data for cyclohexane[47], benzene[48 49] and phenol[44], present predictions and the DIPPR correlations. The results are in a good agreement, i.e. the average absolute deviation of phenol data with respect to the results of the DIPPR correlation is 0.37 l mol^{-1}, while analogous values for cyclohexylamine and aniline are 0.22 and 0.13 l mol^{-1}, respectively.

2.2. Molecular simulation

VLE of the binary systems were calculated by the grand equilibrium method[34], in which the pressure dependence of the chemical potentials of the liquid phase $\mu_i^L(T, p, x_1)$ is estimated by a first order Taylor expansion based on simulation results. In a standard grand equilibrium simulation, the vapor properties are the result of a molecular simulation run in the pseudo grand canonical (μVT) ensemble as fully explained elsewhere[34]. In the present study, the chemical potential of the vapor phase was estimated instead on the basis of the second virial coefficient $B = y_1 B_{11} + 2y_1 y_2 B_{12} + y_2^2 B_{22}$ by $\mu_i^V = \ln(y_i \rho) + 2\rho(y_1 B_{i1} + y_2 B_{i2})$. This approach has statistical advantages because very low density states, as in case of the present three mixtures, can be difficult to sample by Monte Carlo methods[40].

According to Gibbs' phase rule, two variables have to be specified for the VLE of a binary system. Specifying temperature T and molar fraction of the liquid phase x_1, the chemical potentials of the liquid phase μ_i^L can be sampled by molecular simulation and the second virial coefficients B_{ij} can be sampled by integrating Mayer's f function, as in Ref[23]. Pressure and density of the vapor phase are given by $p = \rho kT(1 + B\rho)$ and $\rho = \left[\sqrt{(4Bp/kT) + 1} - 1\right]/2B$, respectively. The pressure and molar fraction of the saturated vapor phase were calculated by solving the non-linear system of equations given by the chemical potentials of the vapor and liquid phases, assuming the equality $\mu_i^L = \mu_i^V$ next to thermal and mechanical equilibrium.

2.3. COSMO-SAC model

The COSMO-SAC model was combined with the PRSV EOS through the Wong-Sandler mixing rule for the prediction of binary VLE. The Wong-Sandler mixing rule[50] [51] was used to determine the energy and volume parameters for the mixtures

$$\frac{a_m}{b_m} = \sum_{i=1}^{2} x_i \frac{a_i}{b_i} + \frac{g^E}{C_{WS}}, \tag{2}$$

$$b_m - \frac{a_m}{RT} = \sum_{i=1}^{2}\sum_{j=1}^{2} \frac{x_i x_j}{2}\left[\left(b_i - \frac{a_i}{RT}\right) + \left(b_j - \frac{a_j}{RT}\right)\right], \tag{3}$$

where $C_{WS} = -\ln\left(1 + \sqrt{2}\right)/\sqrt{2}$ is a constant and the excess Gibbs energy g^E was obtained from the COSMO-SAC model. Two versions of the COSMO-SAC model were investigated

here: COSMO-SAC (2010)[18] and COSMO-SAC (dsp)[52]. The only difference between these two versions is that the dispersion contribution to the activity coefficient is considered by a one-constant Margules equation in the COSMO-SAC (dsp) model. The predictive results from these two methods are almost identical (with a difference below 0.1 %) for all binary mixtures considered in the present work. Therefore, only the results of COSMO-SAC (2010) are presented and this approach is simply denoted as PRSV+WS+COSMOSAC in the following.

2.4. Cubic equation of state

The PRSV EOS[53] describes the pressure-volume-temperature (pvT) relationship by

$$p = \frac{RT}{v-b} - \frac{a}{v^2+2bv-b^2}, \tag{4}$$

where the energy parameter a the and volume parameter b are determined from critical temperature T_c, critical pressure p_c and acentric factor ω by

$$a = 0.457235\frac{R^2T_c^2}{p_c}\left[1+\kappa\left(1-\sqrt{\frac{T}{T_c}}\right)\right]^2, \tag{5}$$

$$b = 0.077796\frac{RT_c}{p_c}, \tag{6}$$

$$\kappa = \kappa_0 + \kappa_1 \left(1 + \sqrt{\frac{T}{T_c}}\right)\left(0.7 - \frac{T}{T_c}\right), \text{for } T < T_c \,, \tag{7}$$

$$\kappa = \kappa_0, \text{for } T \geq T_c \,, \tag{8}$$

$$\kappa_0 = 0.378893 + 1.4897153\omega - 0.1713848\omega^2 + 0.0196654\omega^3 \,. \tag{9}$$

κ_1 is an adjustable parameter which can be optimized to experimental vapor pressure data[54]. Values for numerous compounds were reported in the literature, e.g., for cyclohexane, benzene and cyclohexanol[53] as well as for phenol and aniline[55]. The parameter κ_1 was determined for cyclohexylamine in this work by fitting equation (2) to experimental vapor pressure data, leading to $\kappa_1 = -0.0988$.

The PRSV EOS with the van der Waals mixing rule for the energy and volume parameters, i.e. $a_m = \sum_{i=1}^{2}\sum_{j=1}^{2} x_i x_j a_{ij}$ and $b_m = \sum_{i=1}^{2} x_i b_i$, was used as a baseline. It was allowed for a binary interaction parameter in the quadratic mixing rule of the energy parameter, i.e. $a_{ij} = \left(1 - k_{ij}\right)\sqrt{a_{ii}a_{jj}}$. The binary interaction parameter k_{ij} was optimized by means of the Nelder and Mead method[56] to experimental binary VLE data.

3. Results and discussion

3.1. Vapor-liquid equilibria

Molecular simulation results of the VLE were compared with PRSV+WS+COSMOSAC, the PRSV EOS and experimental data. Figure 8 shows the results for the binary mixture cyclohexane + benzene at 298.15, 323.15 and 403.15 K. The molecular simulation results are in good agreement with the experimental data for this system. It exhibits an azeotropic behavior with a pressure maximum, which is described with molecular simulation by fitting the binary parameter ξ of the modified Lorentz-Berthelot mixing rules

$$\sigma_{ab} = \frac{\sigma_a + \sigma_b}{2}, \tag{10}$$

$$\varepsilon_{ab} = \xi\sqrt{\varepsilon_a \varepsilon_b}\,. \tag{11}$$

The value $\xi = 0.993$, which is only slightly different from the predictive case $\xi = 1$, was obtained by means by adjustment to the experimental vapor pressure. The PRSV EOS is not able to predict the VLE behavior of this mixture and the binary parameter of the quadratic mixing rule $k_{ij} = 0.027$ was optimized by means of the Nelder and Mead method [56].

Figure 9 shows the VLE of the binary mixture cyclohexanol + phenol at 403.35 and 433.25 K. At these temperatures, no experimental data were reported for the saturated vapor phase composition, however, the results by PRSV+WS+COSMOSAC and molecular simulation mutually agree. This system exhibits an azeotropic behavior with a pressure minimum, a behavior described by molecular simulation by increasing the adjustable parameter ξ of the modified Lorentz-Berthelot combination rules. Molecular simulation results with $\xi = 1.07$ are in good agreement with the experimental data reported for this system. The PRSV EOS without a fitted binary parameter $k_{ij} = -0.076$ of the quadratic mixing rule is not able to adequately describe the phase behavior for this system.

Figure 10 shows the VLE of the binary system cyclohexylamine + aniline at 333.15 and 363.15 K that exhibits zeotropic behavior. Molecular simulation quantitatively describes the phase behavior of this system with $\xi = 1.04$ in the modified Lorentz-Berthelot combination rules, which was determined by fitting to the experimental vapor pressure. The calculation results from the PRSV EOS with fitted parameter $k_{ij} = -0.031$ and the prediction results from PRSV+WS+COSMOSAC are shown as well and both results are in good agreement with experimental data.

3.2. Excess properties of the liquid phases

Interactions between molecules can be studied on the basis of the excess properties[57]. In order to explain the change of shape of the phase envelope upon addition of a functional group, the excess volume $v^E = v^{Mix} - (x_1 v_1^0 + x_2 v_2^0)$ and excess enthalpy $h^E = h^{Mix} - (x_1 h_1^0 + x_2 h_2^0)$ and of the liquid phases were examined for the three systems in the entire molar fraction range. v_i^0 and h_i^0 are the volume and enthalpy of the pure component i at the same aggregation state, temperature and pressure as the mixture. It was assumed that the excess properties are not strongly pressure dependent because the excess properties of liquids primarily depend on temperature and composition[58]. Moreover, the pressure variations along the saturated liquid lines are small in absolute terms (below 0.04 MPa). The excess Gibbs energy $g^E = g^{Mix} - (x_1 \mu_1^0 + x_2 \mu_2^0) - RT[x_1 \ln(x_1) + x_2 \ln(x_2)]$ of the saturated liquid phase was considered in the same way as well. Specifying temperature and molar fraction, molecular simulations with the Monte Carlo method were carried out for the saturated liquid phase in the NpT ensemble at the corresponding saturated vapor pressure.

The results for excess Gibbs energy, excess volume and excess enthalpy from molecular simulation, PRSV+WS+COSMOSAC, PRSV EOS and available experimental data are compared in Figure 11. In general, all approaches provide excess enthalpy and excess Gibbs energy with similar magnitudes. However, the excess volume from PRSV+WS+COSMOSAC is much larger than that from PRSV EOS. It has been shown that the quadratic composition dependence of the second virial coefficient (used in the Wong-Sandler mixing rule) provides a larger excess volume with a correct sign when comparing with the quadratic composition dependence of the volume parameter (used in van der Waals mixing rule)[59].

As shown in Figure 11, all three approaches show a clear difference of the excess volume and excess enthalpy between the system without functional group and the hydroxylated and aminated systems. The binary system without functional group exhibits a maximum for both excess enthalpy and excess volume. These results suggest that the isothermal mixing process requires energy to occur (endothermic mixing), which can be attributed to poor packing of unlike molecules, which results in weakening of the intermolecular interactions. Simulation results for the excess properties of equimolar cyclohexane + benzene are reported in Table 3 at 298.15 and 403.15 K. The excess volume increases and the excess enthalpy decreases with increasing temperature.

On the other hand, the hydroxylated and aminated systems exibit a minimum both for excess volume and excess enthalpy, which is related to dominating attractive interactions and their isothermal mixing process has to liberate energy to occur (exothermal mixing). The magnitude of the excess enthalpy reflects that in the case of the hydroxylated system, the unlike attractive interactions are more important than in the aminated system. E.g.

according to the numerical data reported in Table 3, the excess volume increases by 24% in the case of the hydroxylated mixture and 17% in the case of the aminated mixture, taking into account that the increase in temperature is identical for both mixtures ($\Delta T = 30$ K). In addition, the simulation results show that for the hydroxylated and amined systems, the excess enthalpy increases with temperature.

In a diagram according to Smith et al.[58], where g^E/RT is plotted over h^E/RT, six regions can be identified, depending on the sign of the excess properties, cf. Figure 12. The diagonal line represents $s^E/R = 0$ and regions (1) and (4) are dominated by the excess enthalpy, while regions (3) and (6) are dominated by the excess entropy. According to the molecular simulation results shown in Figure 12, the aminated and hydroxylated mixtures reside mainly in region (4), which is dominated by excess enthalpy. Furthermore, there is a clear tendency to the region dominated by the enthalpy for increasing temperature for the system without functional group, i.e. the results tend to move from region (2) toward region (1), which is dominated by excess enthalpy when the temperature is increased.

3.3. Radial distribution functions

The RDF $g_{\alpha-\beta}(r)$ stands for the normalized probability of occurrence of a site of type β at a distance r from a site of type α[24] and is a measure to characterize the microscopic structure of matter. RDF of the saturated liquid mixtures and number integrals for hydrogen bonding systems were determined with Monte Carlo simulations in the NpT ensemble containing 1000 molecules to elucidate the extent of nonrandom mixing[60].

Figure 13 shows the influence of temperature and composition on the RDF of cyclohexane + benzene. Molecular simulation results suggest that there is a very weak coordination shell for this system that barely changes under the varying conditions. The hydroxylated mixture shows a typical hydrogen bonding pattern, cf. Figure 14. The peaks of $g_{\mathrm{O-H}}(r)$ are higher for cyclohexanol-cyclohexanol interactions than those between cyclohexanol-phenol and phenol-phenol, respectively. The first solvation shell is affected by temperature increase and the O-H coordination shell is not dependent on composition at the highest temperature. Moreover, the simulation results suggest that the O-H association pattern of the cyclohexanol-phenol interaction is between the ones of cyclohexanol-cyclohexanol and phenol-phenol. It is clear that the association pattern is much stronger between the aliphatic hydroxyl sites than between the aromatic ones. In the case of the amined system, the opposite occurs as can be seen in Figure 15, i.e. the association pattern for aromatic amine sites is stronger than for aliphatic sites. In addition, the simulation results suggest that the association pattern of aniline-aniline is not strongly affected by increasing temperature. The first coordination shell for cyclohexylamine-aniline, which is located at ~1.7 Å, tends to disappear with increasing temperatue. The association pattern obtained for cyclohexylamine is qualitatively similar to the one of cyclohexane, cf. Figure 13 (left), when the molar fraction of cyclohexylamine is increased.

4. Conclusions

Three different approaches, i.e. molecular simulation, the Peng-Robinson-Stryjek-Vera (PRSV) EOS and the COSMO-SAC model combined with PRSV EOS through the Wong-Sandler mixing rule (PRSV+WS+COSMOSAC), were used to study three binary mixtures, i.e.

cyclohexane + benzene, cyclohexanol + phenol and cyclohexylamine + aniline. Molecular simulations were carried out by means of the grand equilibrium method in a variant relying on the second virial coefficient for the vapor phase and by using force fields for benzene, cyclohexane and cyclohexanol published in previous works by our group. New force fields for cyclohexylamine, phenol and aniline were devised here on the basis of quantum chemical information and pure substance VLE data. The VLE of the pure substances obtained with the new force fields are in quantitative agreement with the available experimental data.

Molecular simulation, the COSMO-SAC model and the PRSV EOS describe the VLE of the three binary mixtures well. These approaches cover the azeotropic behavior in the case of cyclohexane + benzene (with maximum vapor pressure), cyclohexanol + phenol (with minimum vapor pressure) and the zeotropic behavior of the aminated system in a quantitative way. The excess contributions to volume, enthalpy and Gibbs energy were studied along the saturated liquid line. Simulation results showed that the repulsive interactions dominate in case of cyclohexane + benzene, whereas in the other mixtures the attractive interactions dominate. This leads to a positive excess volume in case of the cyclohexane + benzene and to a negative excess volume in case of the functionalized mixtures. However, the attractive interactions are stronger in case of the hydroxylated system than in case of the aminated one. This is reflected by the excess enthalpy, i.e. cyclohexane + benzene is endothermal, whereas the other two mixtures are exothermal.

Azeotropic or zeotropic behavior is mainly governed by the excess Gibbs energy. The mixture without functional group possesses azeotropic behavior with a maximum vapor pressure and positive values of the excess Gibbs energy. The hydroxylated mixture possesses azeotropic

behavior with minimum vapor pressure and negative excess Gibbs energy. The zeotropic mixture, i.e. the aminated system, exhibits excess Gibbs energy values which are closer to zero.

The microscopic structure of the saturated liquids was studied on the basis of molecular force fields. There is a very weak coordination shell in cyclohexane + benzene and a typical hydrogen bonding behavior was found in case of the hydroxylated system. A weaker association pattern is present in the amined system.

Table 1.

Force field parameters for phenol, cyclohexylamine and aniline developed in this work.

Site	*x* / Å	*y* / Å	*z* / Å	*σ* / Å	*ε/κ* / K	*q* / e
Phenol						
CH(1)	-0.3341	2.6368	0	3.282	96.9	0
CH(2)	-0.9511	4.2308	0	3.282	96.9	0
CH(3)	-2.6400	4.4935	0	3.282	96.9	0
CH(4)	-3.7120	3.1622	0	3.282	96.9	0
CH(5)	-3.0950	1.5681	0	3.282	96.9	0
C	-1.4060	1.3054	0	3	95.089	+0.2232
O	-0.9733	0	0	3.149	85.053	-0.5501
H	0	0	0	0	0	+0.3269
Cyclohexylamine						
CH_2(1)	0	0	0	3.477	86.01	0
CH_2(2)	-1.9010	0	0	3.477	86.01	0
CH_2(3)	-1.9011	2.7744	1.4623	3.477	86.01	0
CH_2(4)	-0.0003	2.7747	1.4625	3.477	86.01	0
CH_2(5)	0.6864	1.0022	1.4627	3.477	86.01	0
CH	-2.5873	1.7725	0	3.195	59.88	+0.3052
N	-4.0510	1.7186	-0.0417	3.310	141.863	-0.7804
H(1)	-4.3836	1.3018	0.8276	0	0	+0.2626
H(2)	-4.4079	2.6725	-0.0929	0	0	+0.2126

Aniline						
CH(1)	-1.7127	0	0	3.28	80	0
CH(2)	-2.5691	1.4832	0	3.28	80	0
CH(3)	-1.7127	2.9665	0	3.28	80	0
CH(4)	0	2.9665	0	3.28	80	0
CH(5)	0.8563	1.4832	0	3.28	80	0
C	0	0	0	3.35	105	+0.154
N	0.6833	-1.2143	-0.0504	3.315	142.147	-0.800
H(1)	1.6026	-1.1794	0.3305	0	0	+0.323
H(2)	0.1764	-1.9819	0.3307	0	0	+0.323

Table 2.

Critical point from the present force fields for phenol, cyclohexylamine and aniline compared with experimental data.

Substance	Ref.	T_c / K	p_c / MPa	ρ_c / mol l^{-1}
Phenol	This work	701	5.6	3.7
	[44] [45]	694.25	5.93	4.3668
Cyclohexylamine	This work	608.2	3.9	2.9
	[46] (a)	615	4.20	2.28
Aniline	This work	693.8	4.74	3.48
	[44]	699	5.31	3.699

(a) Predicted value

Table 3.

Excess properties of equimolar mixtures at different temperatures.

Mixture	T / K	v^E / $\mathrm{cm^3\ mol^{-1}}$	h^E / $\mathrm{kJ\ mol^{-1}}$	g^E / $\mathrm{kJ\ mol^{-1}}$
Cyclohexane + benzene	298.15	0.408 ± 0.006	0.644 ± 0.002	0.777 ± 0.10
	403.15	0.671 ± 0.012	0.518 ± 0.003	0.354 ± 0.07
Cyclohexanol + phenol	403.35	-1.160 ± 0.060	-1.522 ± 0.005	-1.019± 0.010
	433.25	-1.437 ± 0.070	-1.578 ± 0.005	-1.242± 0.084
Cyclohexylamine + aniline	333.15	-1.061 ± 0.005	-1.055 ± 0.003	-0.559 ± 0.08
	363.15	-1.246 ± 0.007	-1.072 ± 0.003	-0.505 ± 0.07

Figure captions

Figure 1 Workflow of the present force field parameterization process.

Figure 2 Force field structures for cyclohexane (a), benzene (b), cyclohexanol (c), phenol (d), cyclohexylamine (e) and aniline (f): Orange sites represent methyl groups, yellow sites represent methylene groups, white sites represent hydrogen atoms, blue sites represent nitrogen atoms and red sites represent oxygen atoms.

Figure 3 Saturated densities: Present molecular simulation results for cyclohexane (○), benzene (△), cyclohexanol (□), phenol (green triangles), cyclohexylamine (red squares) and aniline (blue circles) are compared with experimental data (corresponding cross symbols) for cyclohexane[61 62 63], benzene[64], cyclohexanol[65], phenol[44], aniline[66] and cyclohexylamine[65]. Solid lines represent the results from equations of state for benzene by Thol et al.[38] and cyclohexane by Zhou et al.[39] as well as the DIPPR correlations[37] for the remaining substances.

Figure 4 Clausius-Clapeyron plots: Present molecular simulation results for cyclohexane (○), benzene (△), cyclohexanol (□), phenol (green triangles), cyclohexylamine (red squares) and aniline (blue circles) are compared with experimental data (corresponding cross symbols) for cyclohexane[67 68], benzene[69], cyclohexanol[70], phenol[71 72], cyclohexylamine[73 74] and aniline[75 76]. Solid lines represent the results from equations of state for benzene by Thol et al.[38] and cyclohexane by Zhou et al.[39] as well as the DIPPR correlations[37] for the remaining substances.

Figure 5 Enthalpy of vaporization: Present molecular simulation results for cyclohexane (○), benzene (△), cyclohexanol (□), phenol (green triangles), cyclohexylamine (red squares) and aniline (blue circles) are compared with experimental data (corresponding cross symbols) for cyclohexane[77 78], benzene[78], phenol, cyclohexylamine[41 42]. Solid lines represent the results from equations of state for benzene by Thol et al.[38] and cyclohexane by Zhou et al.[39] as well as the DIPPR correlations[37] for the remaining substances.

Figure 6 Second virial coefficient: Present results for cyclohexane (○), benzene (△), cyclohexanol (□), phenol (green triangles), cyclohexylamine (red squares) and aniline (blue circles) based on the according force fields are compared with experimental data (corresponding cross symbols) for cyclohexane[47], benzene[48 49] and phenol[44]. Lines represent the DIPPR correlations[37] for phenol, cyclohexylamine, aniline and cyclohexanol. For cyclohexane the equation of state by Zhou et al. [39] and for benzene by Thol et al. [38] is shown.

Figure 7 Relative deviations ($\delta z = 100(z - z_{corr})/z_{corr}$) of vapor-liquid equilibrium properties for phenol (green triangles), cyclohexylamine (red squares) and aniline (blue circles) from the DIPPR correlations together with experimental data (corresponding cross symbols).

Figure 8 Vapor-liquid equilibria of cyclohexane + benzene: Blue lines represent predictive results of the PRSV EOS $(k_{ij} = 0)$, red lines represent results of the fitted PRSV EOS $(k_{ij} = 0.027)$. Black lines represent predictions with PRSV+WS+COSMOSAC, black circles represent molecular simulation results with $\xi = 0.993$ in the modified Lorentz-Berthelot combination rules and crosses represent experimental data at 298.15 K [1], 323.15 K [2] and 403.15 K [3].

Figure 9 Vapor-liquid equilibria of cyclohexanol + phenol: Blue lines represent predictive results from the PRSV EOS $(k_{ij} = 0)$, red lines represent results of the fitted PRSV EOS $(k_{ij} = -0.076)$. Black lines represent predictions with PRSV+WS+COSMOSAC, black circles represent molecular simulation results with $\xi = 1.07$ in the modified Lorentz-Berthelot combination rules and crosses represent experimental data[4].

Figure 10 Vapor-liquid equilibria of cyclohexylamine + aniline: Blue lines represent predictive results from the PRSV EOS $(k_{ij} = 0)$, red lines represent results of the fitted PRSV EOS $(k_{ij} = -0.031)$. Black lines represent predictions with PRSV+WS+COSMOSAC, black circles represent molecular simulation results with $\xi = 1.04$ in the modified Lorentz-Berthelot combination rules and crosses represent experimental data[5].

Figure 11 Excess enthalpy, excess Gibbs energy and excess volume of cyclohexane + benzene (left), cyclohexanol + phenol (center) and cyclohexilamine + aniline (right) along the saturated liquid line: White and black squares represent simulation data at low and high temperatures, respectively, i.e. 298.15 and 403.15 K for cyclohexane + benzene, 403.35 and 433.25 K for cyclohexanol + phenol and 333.15 and 363.15 K for cyclohexylamine + aniline. Red and black lines represent results by PRSV EOS and PRSV+WS+COSMOSAC, respectively, at same high (solid lines) and low temperatures (dashed line). Blue crosses represent available experimental data, i.e. excess enthalpy[79] and excess volume[80] at 298.15 K for cyclohexane + benzene, excess enthalpy[81] at 318.15 K for cyclohexanol + phenol and excess volume[82] at 303.15 K for cyclohexylamine + aniline.

Figure 12 Excess enthalpy over excess Gibbs energy diagram of the saturated liquid mixtures from molecular simulation: Squares (green for 298.15 K, yellow for 323.15 K and red for

403.15 K) represent results for cyclohexane + benzene. Triangles (green for 403.35 K and yellow for 433.25 K) represent results for cyclohexanol + phenol and circles (green for 333.15 K and yellow for 363.15 K) represent results for cyclohexylamine + aniline.

Figure 13 Radial distribution functions in the saturated liquid state between CH_2-CH_2, CH_2-CH and CH-CH sites of cyclohexane-cyclohexane, cyclohexane-benzene and benzene-benzene at different temperatures and compositions: Black lines represent the molecular simulation results with α=CH_2 and β=CH_2, blue lines represent the molecular simulation results with α=CH_2 and β=CH and red lines represent molecular simulation results with α=CH and β=CH. Dotted lines are results with x_{C6H12}=0.1 mol/mol, short dashed lines are results with x_{C6H12}=0.5 mol/mol and solid lines with x_{C6H12}=0.9 mol/mol. Plots (c), (f) and (i) are results at 298.15 K, (b), (e) and (h) at 323.15 K and (a), (d) and (g) at 403.15 K.

Figure 14 Radial distribution functions in the saturated liquid state between O-H sites and number integrals (inset) of cyclohexanol-cyclohexanol (left, black lines), cyclohexanol-phenol (center, red lines) and phenol-phenol (right, blue lines) at different temperatures and compositions: Dotted lines are results with x_{C6H12O}=0.1 mol/mol, short dashed lines are results with x_{C6H12O}=0.5 mol/mol and solid lines with x_{C6H12O}=0.9 mol/mol. Plots (d), (e) and (f) are results at 403.35 K, (a), (b) and (c) at 433.25 K.

Figure 15 Radial distribution functions in the saturated liquid state between N-H sites and number integrals (inset) of cyclohexylamine-cyclohexylamine (left, black lines), cyclohexylamine-aniline (center, blue lines) and aniline-aniline (right, red lines) at different temperatures and compositions: Dotted lines are results with x_{C6H13N}=0.1 mol/mol, short

dashed lines are results with x_{C6H13N}=0.5 mol/mol and solid lines with x_{C6H13N}=0.9 mol/mol. Plots (d), (e) and (f) are results at 333.15 K, (a), (b) and (c) at 363.15 K.

Figure 1

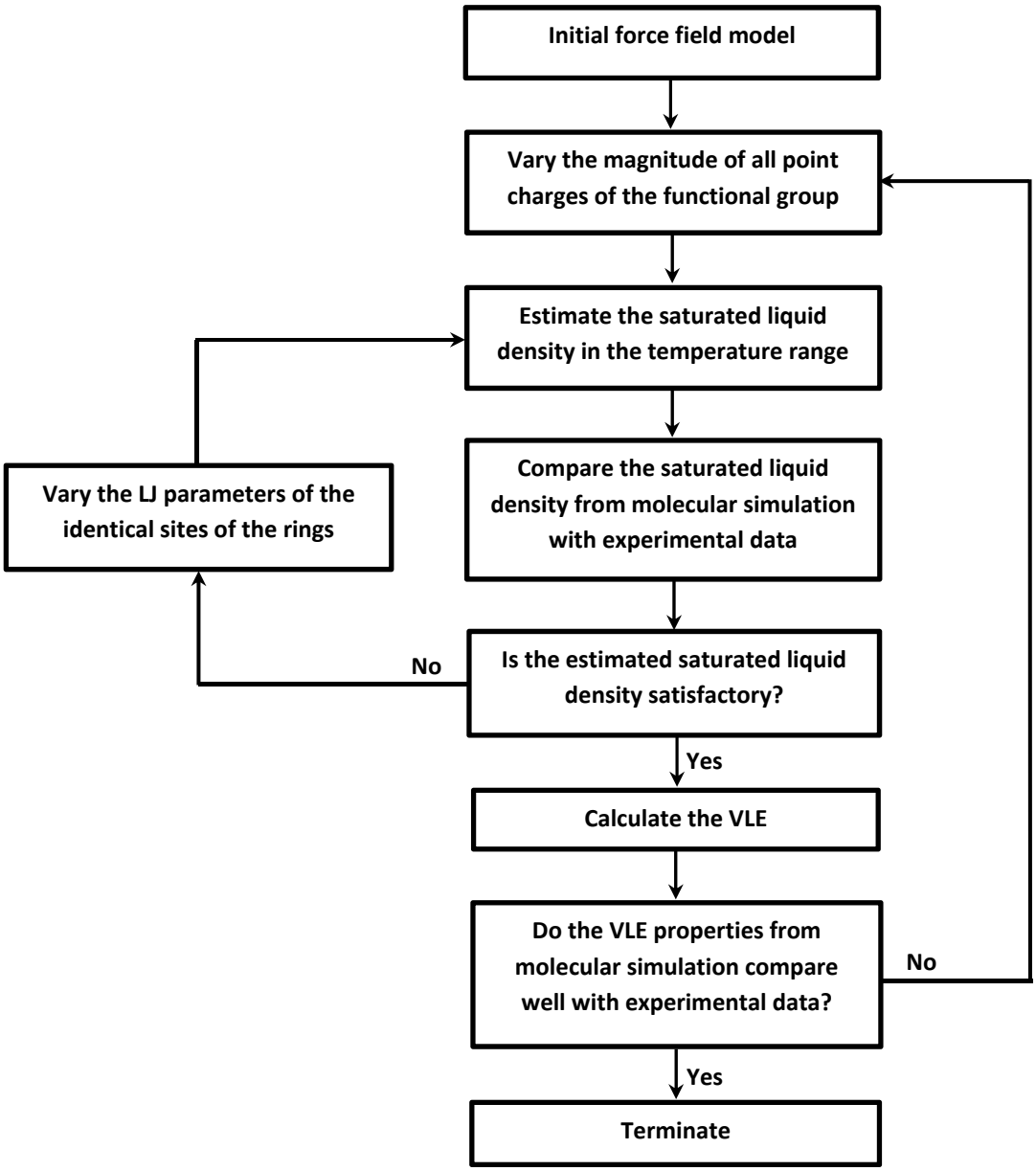
Initial force field model
Vary the magnitude of all point charges of the functional group
Estimate the saturated liquid density in the temperature range
Compare the saturated liquid density from molecular simulation with experimental data
Is the estimated saturated liquid density satisfactory?
No
Vary the LJ parameters of the identical sites of the rings
Yes
Calculate the VLE
Do the VLE properties from molecular simulation compare well with experimental data?
No
Yes
Terminate

Figure 2

(a)

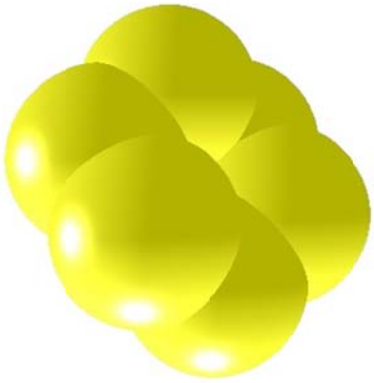

(b)

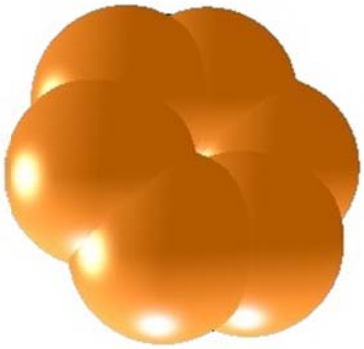

(c)

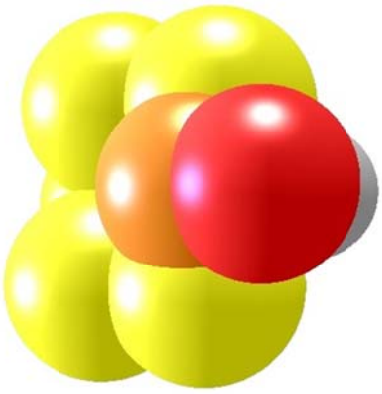

(d)

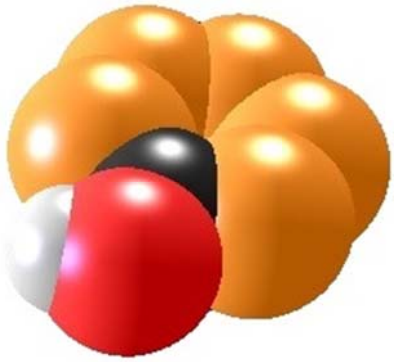

(e)

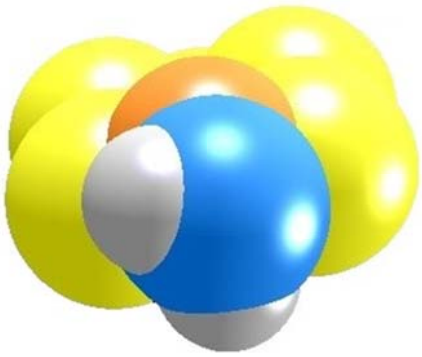

(f)

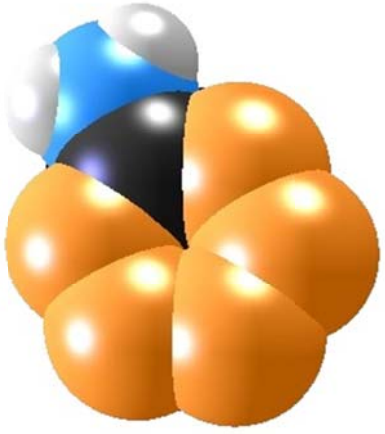

Figure 3

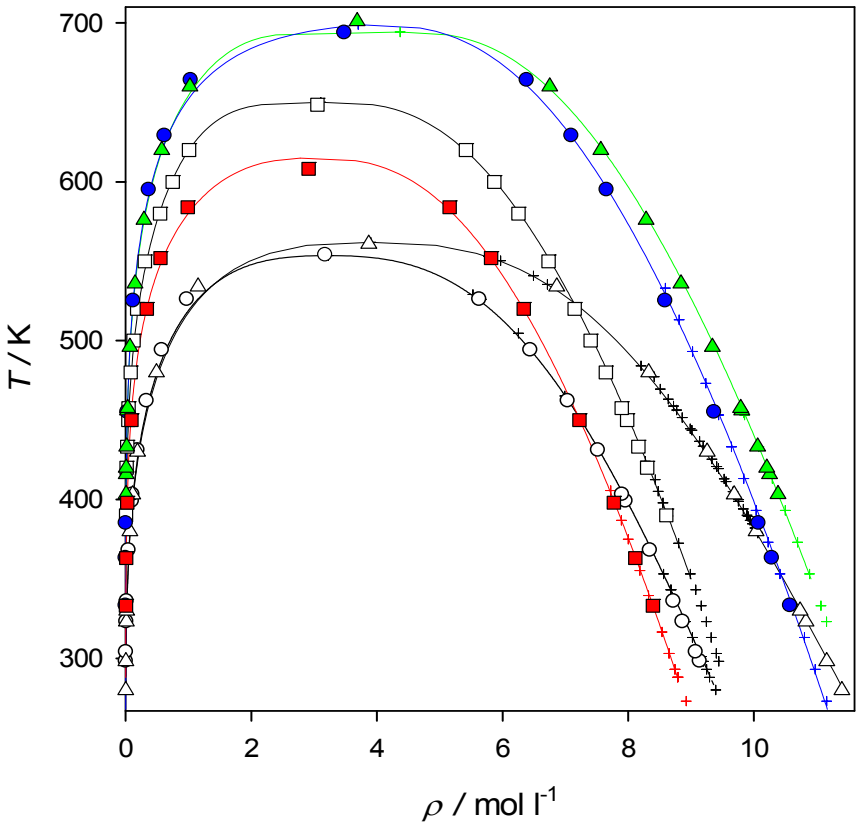

Figure 4

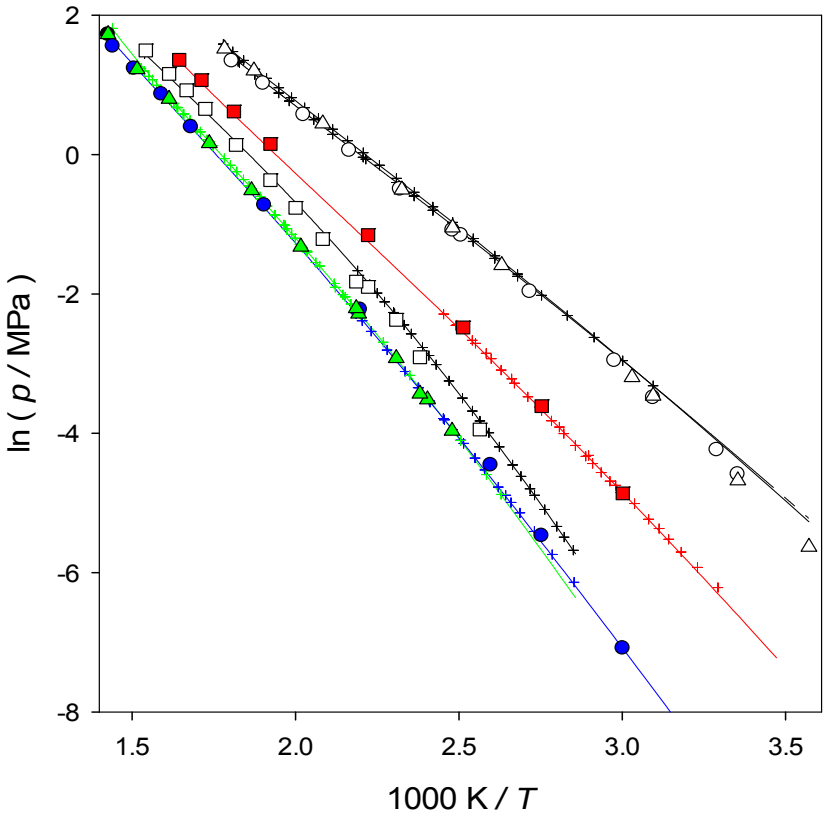

Figure 5

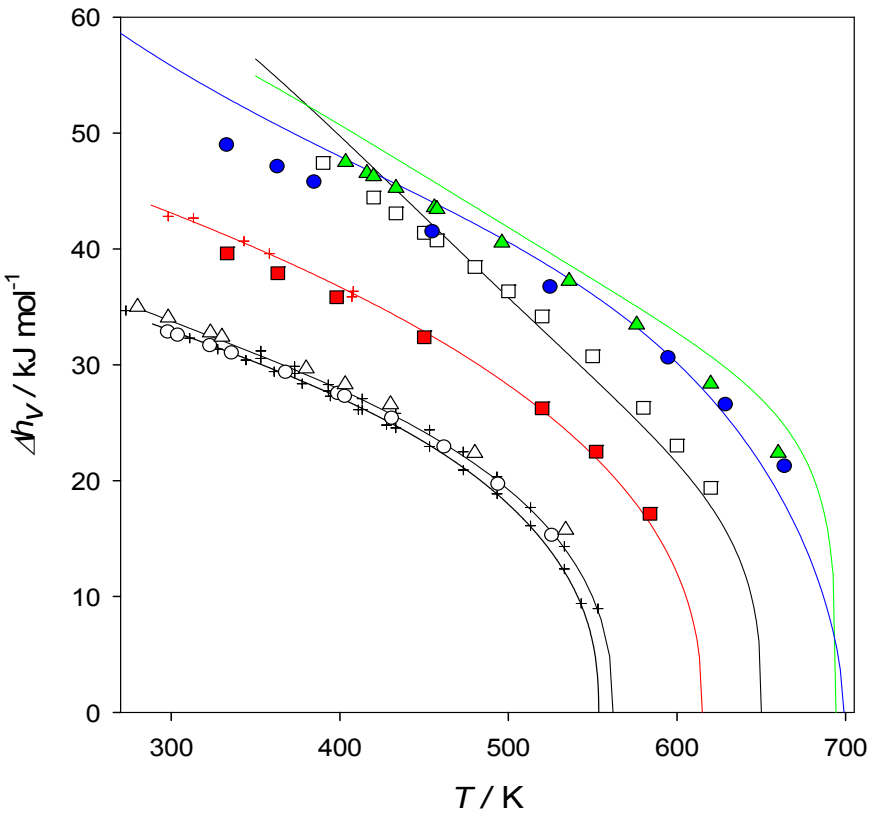

Figure 6

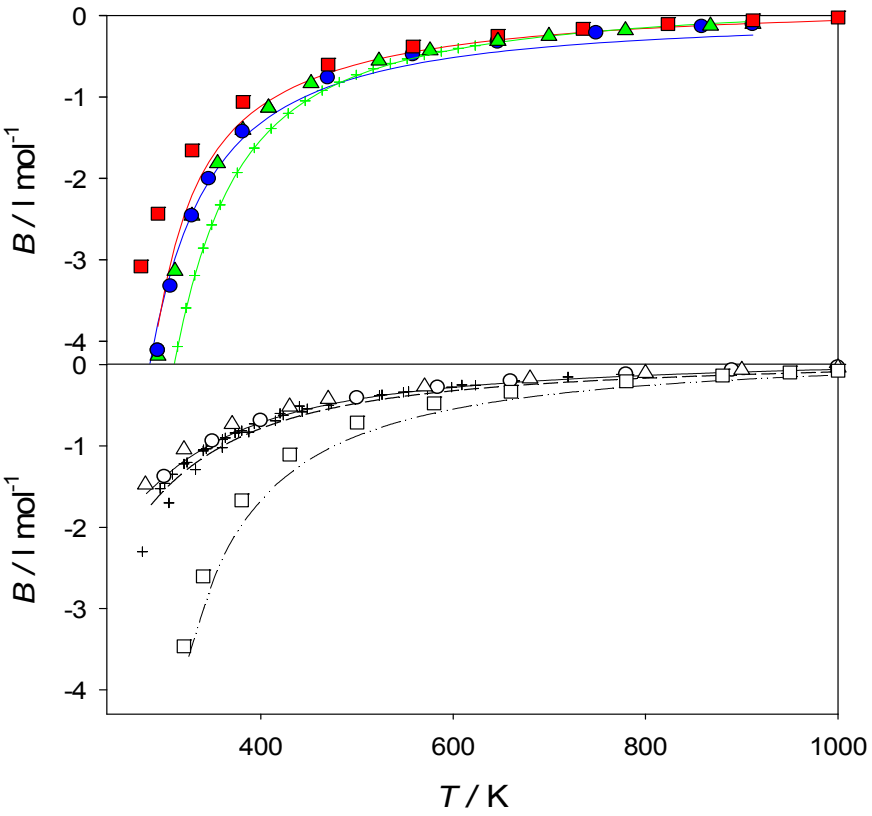

Figure 7

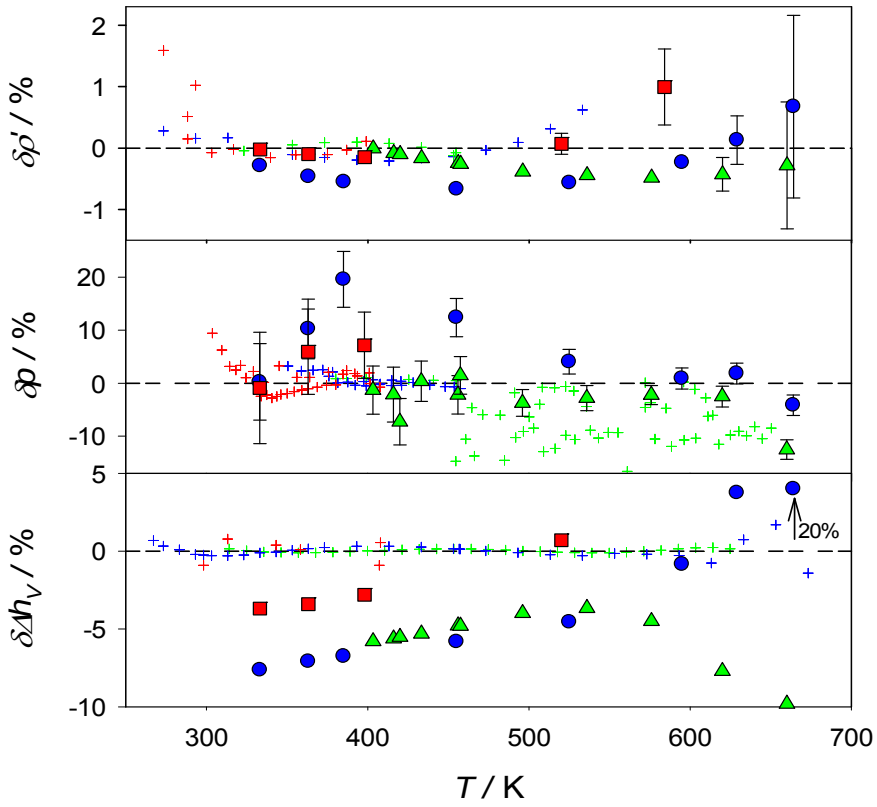

Figure 8

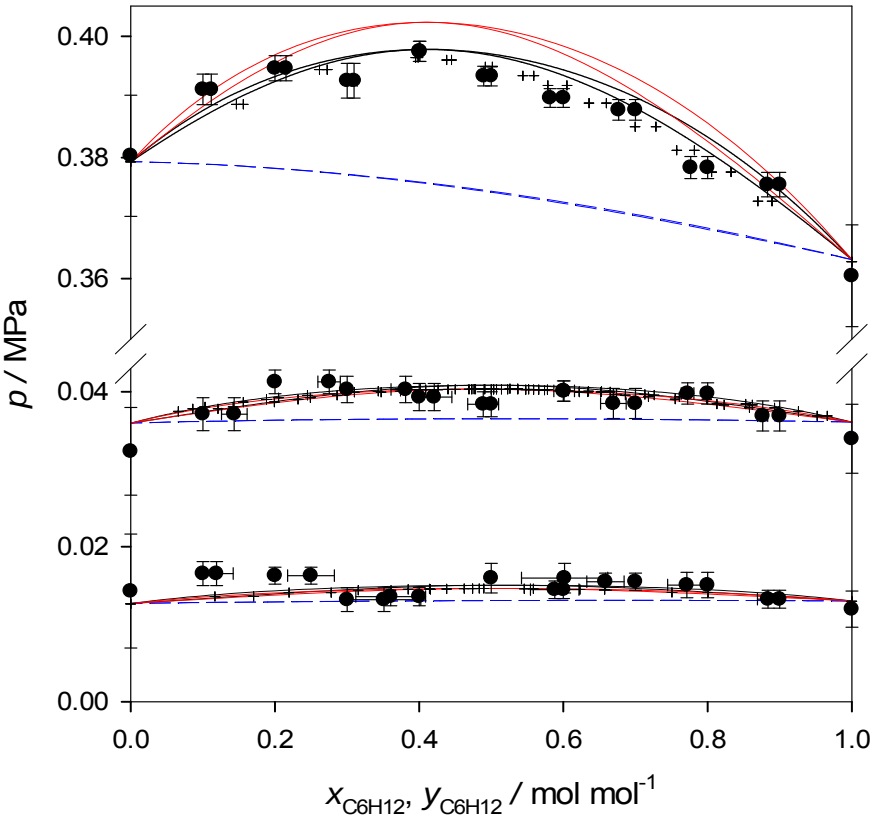
0.40
0.38
0.36
0.04
0.02
0.00
0.0
0.2
0.4
0.6
0.8
1.0
p / MPa
x_C6H12, y_C6H12 / mol mol^-1

Figure 9

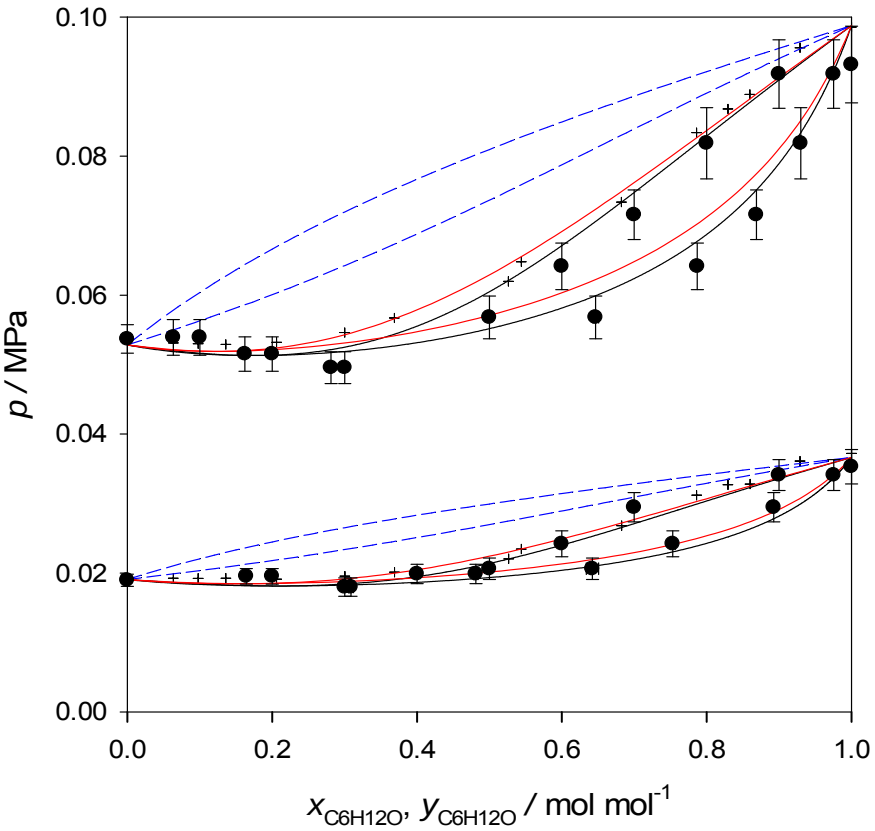
0.10
0.08
0.06
0.04
0.02
0.00
p / MPa
0.0
0.2
0.4
0.6
0.8
1.0
x C6H12O, y C6H12O / mol mol-1

Figure 10

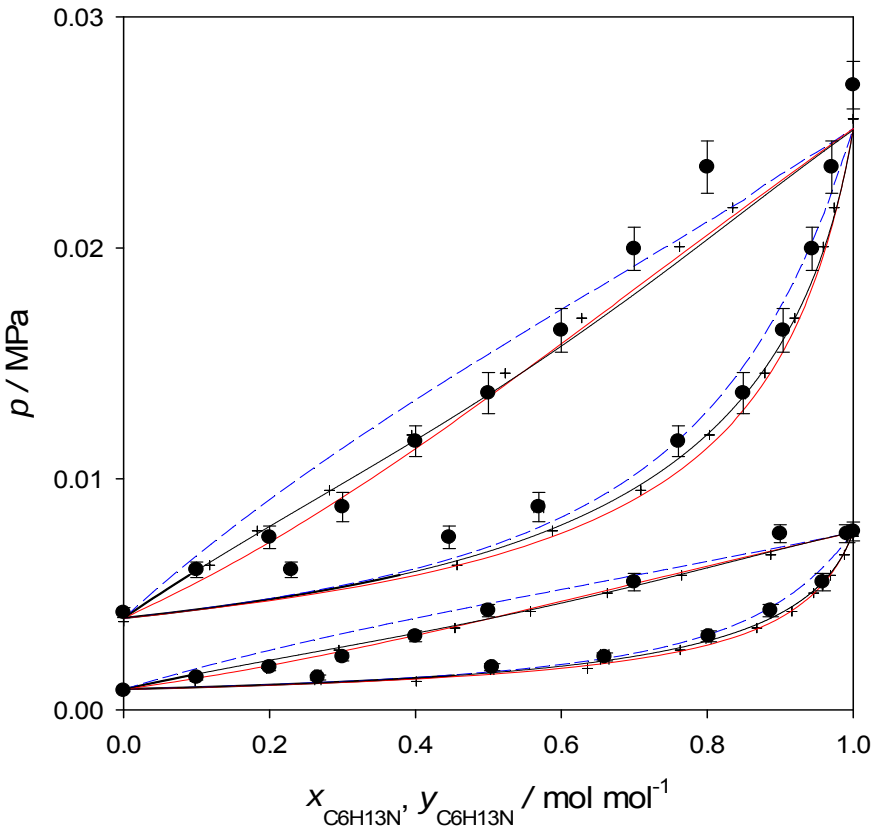

Figure 11

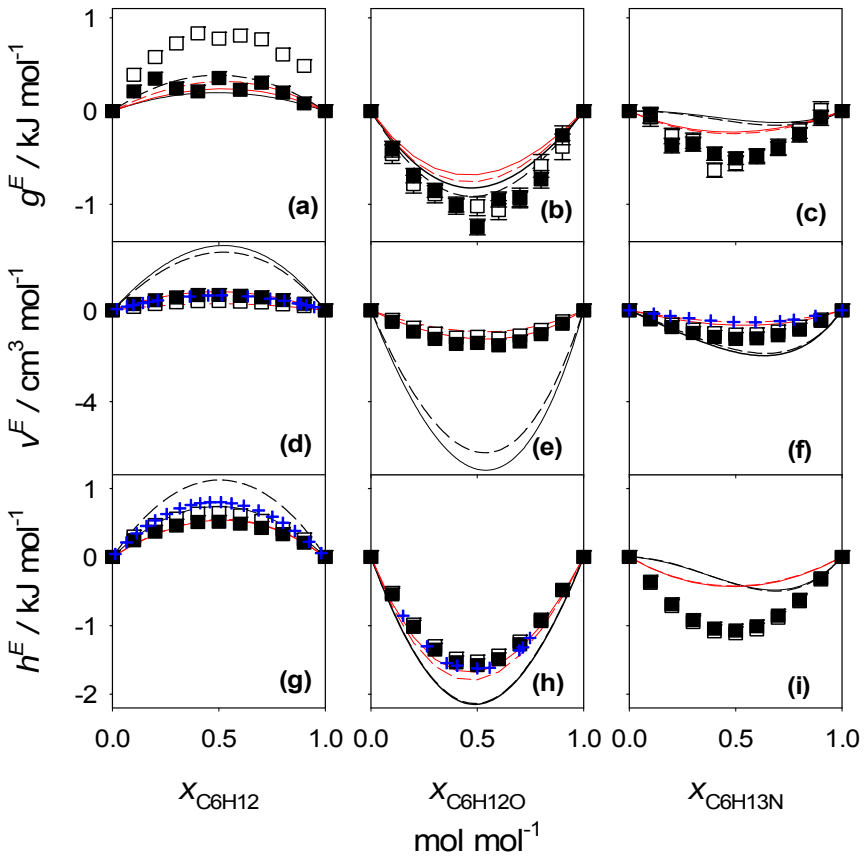
g^E / kJ mol^{-1}
v^E / cm^3 mol^{-1}
h^E / kJ mol^{-1}
(a)
(b)
(c)
(d)
(e)
(f)
(g)
(h)
(i)
x_{C6H12}
x_{C6H12O}
x_{C6H13N}
mol mol^{-1}

Figure 12

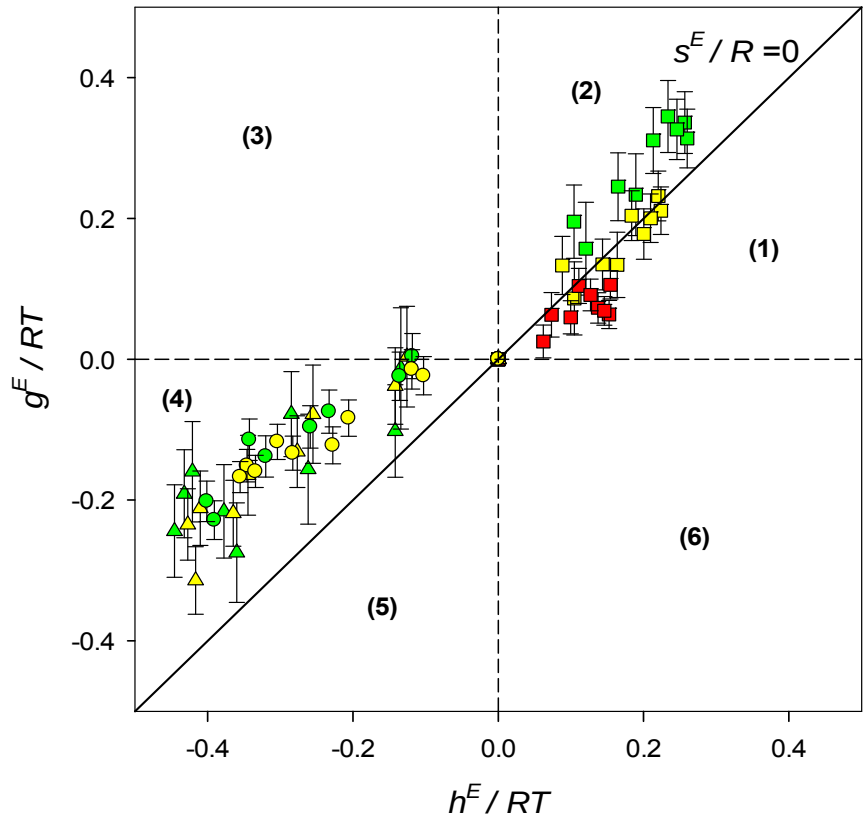

Figure 13

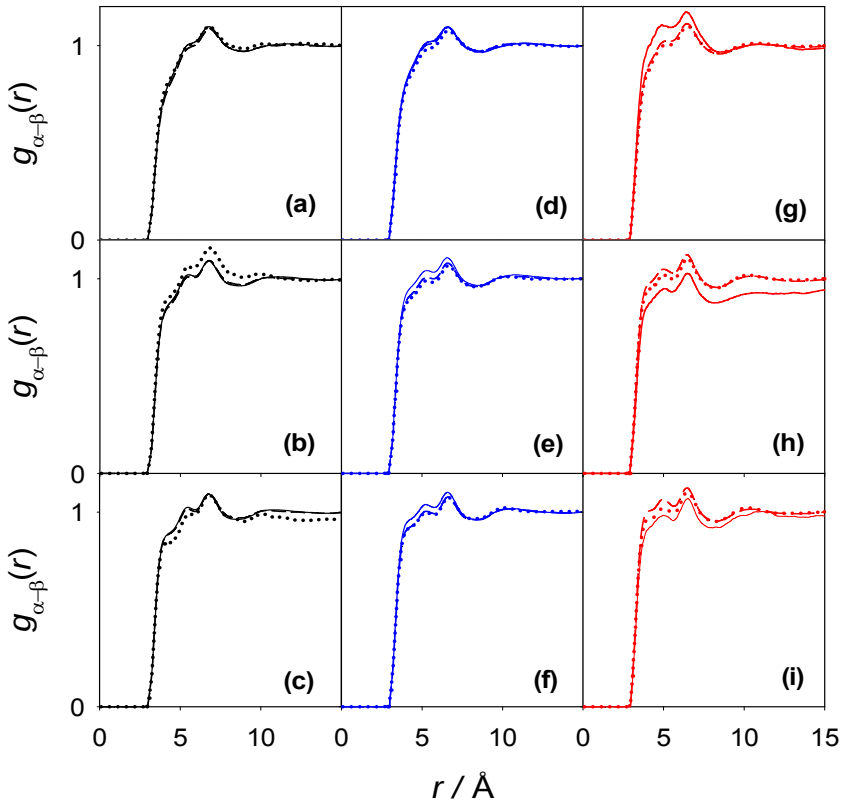

Figure 14

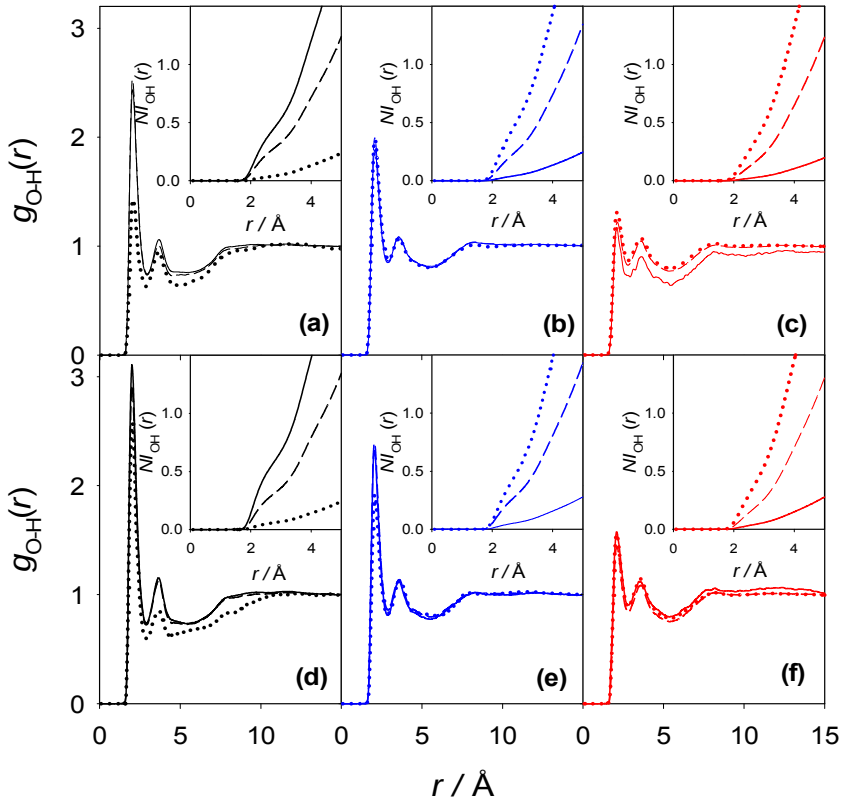

Figure 15

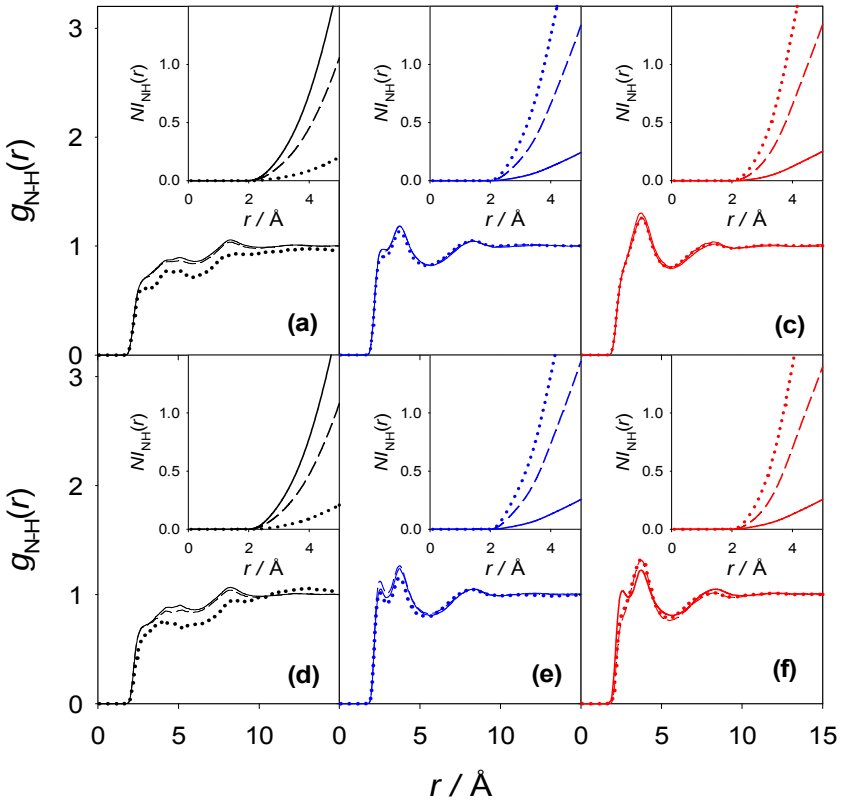

References

(1) Mentzer, R. A.; Greenkorn, R. A.; Chao, K. C. Bubble Pressures and Vapor-Liquid Equilibria for Four Binary Hydrocarbon Mixtures. *J. Chem. Thermodyn.* **1982**, *14* (9), 817–830.

(2) Kiyofumi, K.; Masanori, U.; Kazuo, K. Isothermal Vapor−Liquid Equilibria for Benzene + Cyclohexane + 1-Propanol and for Three Constituent Binary Systems. *J. Chem. Eng. Data* **1997**, *42* (1), 149–154.

(3) Jilian, D.; Chuanzhuang, F.; Yonghong, L. Isothermal Vapor−Liquid Equilibrium for Methanol and 2,3-Dimethyl-1-Butene at 343.06 K, 353.27 K, 363.19 K, and 372.90 K. *J. Chem. Eng. Data* **2011**, *56* (5), 2386–2392.

(4) Wobst, M.; Moerke, K. *FIZ Report 6281*; 1990.

(5) Grenner, A.; Klauck, M.; Schmelzer, J. An Equipment for Dynamic Measurements of Vapour-Liquid Equilibria and Results in Binary Systems Containing Cyclohexylamine. *Fluid Phase Equilib.* **2005**, *233* (2), 170–175.

(6) Yamamoto, Y. S. Benzene. In *Ullmann's Encyclopedia of Industrial Chemistry*; VCH Verlagsgesellschaft mbH: Weinheim, 1985.

(7) Yamamoto, Y. S. Cyclohexane. In *Ullmann's Encyclopedia of Industrial Chemistry*; VCH Verlagsgesellschaft mbH: Weinheim, 1985.

(8) Xia, Z.; Lu, H.; Liu, H.; Zhang, Z.; Chen, Y. Cyclohexane Dehydrogenation over Ni-Cu/SiO2 Catalyst: Effect of Copper Addition. *Catal. Commun.* **2017**, *90*, 39–42.

(9) Fang, X.; Yin, Z.; Wang, H.; Li, J.; Liang, X.; Kang, J.; He, B. Controllable Oxidation of Cyclohexane to Cyclohexanol and Cyclohexanone by a Nano-MnOx/Ti Electrocatalytic Membrane Reactor. *J. Catal.* **2015**, *329*, 187–194.

(10) Schuchardt, U.; Cardoso, D.; Sercheli, R.; Pereira, R.; da Cruz, R. S.; Guerreiro, M. C.; Mandelli, D.; Spinacé, E. V.; Pires, E. L. Cyclohexane Oxidation Continues to Be a Challenge. *Appl. Catal. A Gen.* **2001**, *211* (1), 1–17.

(11) Yamamoto, Y. S. Cyclohexanol and Cyclohexanone. In *Ullmann's Encyclopedia of Industrial Chemistry*; VCH Verlagsgesellschaft mbH: Weinheim, 1985.

(12) Chen, B.-C.; Yu, B.-Y.; Lin, Y.-L.; Huang, H.-P.; Chien, I.-L. Reactive-Distillation Process for Direct Hydration of Cyclohexene to Produce Cyclohexanol. *Ind. Eng. Chem. Res.* **2014**, *53* (17), 7079–7086.

(13) Morrison, R. T.; Boyd, R. N. *Organic Chemistry*, 5th ed.; Allyn and Bacon: Boston, 1987.

(14) Ma, D.; Zou, D.; Zhou, D.; Li, T.; Dong, S.; Xu, Z.; Dong, S. Phenol Removal and Biofilm Response in Coupling of Visible-Light-Driven Photocatalysis and Biodegradation: Effect of Hydrothermal Treatment Temperature. *Int. Biodeterior. Biodegrad.* **2015**, *104*, 178–185.

(15) Hao, X.; Pritzker, M.; Feng, X. Use of Pervaporation for the Separation of Phenol from Dilute Aqueous Solutions. *J. Memb. Sci.* **2009**, *335* (1–2), 96–102.

(16) Chatterjee, M.; Sato, M.; Kawanami, H.; Ishizaka, T.; Yokoyama, T.; Suzuki, T. Hydrogenation of Aniline to Cyclohexylamine in Supercritical Carbon Dioxide: Significance of Phase Behaviour. *Appl. Catal. A Gen.* **2011**, *396* (1–2), 186–193.

(17) Kirk-Othmer. Kirk-Othmer Encyclopedia of Chemical Technology. **1997**, *24*, 233–250.

(18) Hsieh, C. M.; Sandler, S. I.; Lin, S. T. Improvements of COSMO-SAC for Vapor-Liquid and Liquid-Liquid Equilibrium Predictions. *Fluid Phase Equilib.* **2010**, *297* (1), 90–97.

(19) Lyu, Z.; Zhou, T.; Chen, L.; Ye, Y.; Sundmacher, K.; Qi, Z. Reprint of: Simulation Based Ionic Liquid Screening for Benzene-Cyclohexane Extractive Separation. *Chem. Eng. Sci.* **2014**, *115*, 186–194.

(20) Grenner, A.; Klauck, M.; Meinhardt, R.; Schumann, R.; Schmelzer, J. Ternary Liquid−Liquid(−Liquid) Equilibria of Aniline + Cyclohexylamine + Water, Aniline + Cyclohexylamine + Octane, Aniline + Water + Toluene, and Aniline + Water + Octane. *J. Chem. Eng. Data* **2006**, *51* (3), 1009–1014.

(21) Kamath, G.; Georgiev, G.; Potoff, J. J. Molecular Modeling of Phase Behavior and Microstructure of Acetone−Chloroform−Methanol Binary Mixtures. *J. Phys. Chem. B* **2005**, *41* (109), 19463.

(22) Eckl, B.; Vrabec, J.; Hasse, H. Set of Molecular Models Based on Quantum Mechanical Ab Initio Calculations and Thermodynamic Data. *J. Phys. Chem. B* **2008**, *112* (40), 12710–12721.

(23) Muñoz-Muñoz, Y. M.; Guevara-Carrion, G.; Llano-Restrepo, M.; Vrabec, J. Lennard-Jones Force Field Parameters for Cyclic Alkanes from Cyclopropane to Cyclohexane. *Fluid Phase Equilib.* **2015**, *404*, 150–160.

(24) Jorgensen, W. L.; Laird, E. R.; Nguyen, T. B.; Tirado-Rives, J. Monte Carlo Simulations of Pure Liquid Substituted Benzenes with OPLS Potential Functions. *J. Comput. Chem.*

1993, *14* (2), 206–215.

(25) Sagarik, K.; Asawakun, P. Intermolecular Potential for Phenol Based on the Test Particle Model. *Chem. Phys.* **1997**, *219* (2–3), 173–191.

(26) Mooney, D. A.; Müller-Plathe, F.; Kremer, K. Simulation Studies for Liquid Phenol: Properties Evaluated and Tested over a Range of Temperatures. *Chem. Phys. Lett.* **1998**, *294* (September), 135–142.

(27) Rai, N.; Siepmann, J. I. Transferable Potentials for Phase Equilibria. 10. Explicit-Hydrogen Description of Substituted Benzenes and Polycyclic Aromatic Compounds. *J. Phys. Chem. B* **2013**, *117* (1), 273–288.

(28) Merker, T.; Vrabec, J.; Hasse, H. Engineering Molecular Models: Efficient Parameterization Procedure and Cyclohexanol as Case Study. *Soft Mater.* **2012**, *10* (1–3), 3–25.

(29) Guevara-Carrion, G.; Janzen, T.; Muñoz-Muñoz, Y. M.; Vrabec, J. Mutual Diffusion of Binary Liquid Mixtures Containing Methanol, Ethanol, Acetone, Benzene, Cyclohexane, Toluene, and Carbon Tetrachloride. *J. Chem. Phys.* **2016**, *144* (12), 124501.

(30) Johnson III, R. D. NIST Computational Chemistry Comparison and Benchmark Database. *NIST Standard Reference, Database Number 101*. 2013, p http://cccbdb.nist.gov/.

(31) Essén, H.; Svensson, M. Calculation of Coordinates from Molecular Geometric Parameters and the Concept of a Geometric Calculator. *Comput. Chem.* **1996**, *20* (4),

389–395.

(32) Guevara-Carrion, G.; Vrabec, J.; Hasse, H. On the Prediction of Transport Properties of Monomethylamine, Dimethylamine, Dimethylether and Hydrogen Chloride by Molecular Simulation. *Fluid Phase Equilib.* **2012**, *316*, 46–54.

(33) Schnabel, T.; Vrabec, J.; Hasse, H. Henry's Law Constants of Methane, Nitrogen, Oxygen and Carbon Dioxide in Ethanol from 273 to 498 K: Prediction from Molecular Simulation. *Fluid Phase Equilib.* **2005**, *233* (2), 134–143.

(34) Vrabec, J.; Hasse, H. Grand Equilibrium: Vapour-Liquid Equilibria by a New Molecular Simulation Method. *Mol. Phys.* **2002**, *100* (21), 3375–3383.

(35) Glass, C. W.; Reiser, S.; Rutkai, G.; Deublein, S.; Köster, A.; Guevara-Carrion, G.; Wafai, A.; Horsch, M.; Bernreuther, M.; Windmann, T.; et al. ms2: A Molecular Simulation Tool for Thermodynamic Properties, New Version Release. *Comput. Phys. Commun.* **2014**, *185* (12), 3302–3306.

(36) Deublein, S.; Eckl, B.; Stoll, J.; Lishchuk, S. V.; Guevara-Carrion, G.; Glass, C. W.; Merker, T.; Bernreuther, M.; Hasse, H.; Vrabec, J. ms2: A Molecular Simulation Tool for Thermodynamic Properties. *Comput. Phys. Commun.* **2011**, *182* (11), 2350–2367.

(37) Rowley, R. L.; Wilding, W. V.; Oscarson, J. L.; Yang, Y.; Zundel, N. A.; Daubert, T. E.; Danner, R. P. *The DIPPR Data Compilation of Pure Chemical Properties*; AIChE: New York, 2007.

(38) Thol, M.; Lemmon, E.; Span, R. Equation of State for Benzene for Temperatures from the Melting Line up to 725 K with Pressures up to 500 MPa. *High Temp. Press.* **2012**,

41 (2), 81–97.

(39) Zhou, Y.; Liu, J.; Penoncello, S. G.; Lemmon, E. W. An Equation of State for the Thermodynamic Properties of Cyclohexane. *J. Phys. Chem. Ref. Data* **2014**, *43* (4), 43105.

(40) Nezbeda, I. Simulations of Vapor-Liquid Equilibria: Routine versus Thoroughness. *J. Chem. data* **2016**, *61* (12), 3964.

(41) Steele, W. V. The Standard Enthalpies of Formation of Cyclohexylamine and Cyclohexylamine Hydrochloride. *J. Chem. Thermodyn.* **1979**, *11* (12), 1185–1188.

(42) Majera, V.; Svobodaa, V.; Koubekb, J.; Picka, I. Temperature Dependence of Heats of Vaporization, Saturated Vapour Pressures and Cohesive Energies for a Group of Amines. *Collect. Czech. Chem. Commun.* **1979**, *44* (12), 3521–3528.

(43) Clapeyron, E. Mémoire Sur La Puissance Motrice de La Chaleur. *L'ecole Polytech.* **1834**, *14* (23), 153–190.

(44) Kudchadker, A. P.; Kudchadker, S. A.; Wilhoit, R. C. *Key Chemicals Data Book: Phenol*; Thermodynamics Research Center, Texas Engineering Experiment Station, Texas A&M University: College Station Texas, 1977.

(45) Delaunois, C. Phenol, 2-, 3-, 4 Methylphenols. *Ann. Mines Belg.* **1968**, *1*, 9–16.

(46) Lydersen, A. L. *Estimation of Critical Properties of Organic Compounds, College Engineering University Wisconsin, Engineering Experimental Station Report 3, Madison, WI, April.*; 1955.

(47) Rossini, F. D. *Selected Values of Physical and Thermodynamic Properties of Hydrocarbons and Related Compounds: Comprising the Tables of the American Petroleum Institute Research Project 44 Extant as of December 31, 1952*; Carnegie Press: Pittsburgh, 1953.

(48) Dymond, J. H.; Smith, E. B. *The Virial Coefficient of Gases: A Critical Compilation*; Clarendon Press: Oxford, 1969.

(49) Beck, E.; Opel, G.; Pietsch, R.; Vogel, E. Second Virial Coefficient and the Viscosity Coefficient of Benzene Vapor and Their Representability by Lennard-Jones-(M-N) Equations for Intermolecular Potential. *Z. Phys. Chem* **1979**, *260* (6).

(50) Wong, D. S. H.; Sandler, S. I. A Theoretically Correct Mixing Rule for Cubic Equations of State. *AIChE J.* **1992**, *38* (5), 671–680.

(51) Wong, D. S. H.; Orbey, H.; Sandler, S. I. Equation of State Mixing Rule for Nonideal Mixtures Using Available Activity Coefficient Model Parameters and That Allows Extrapolation over Large Ranges of Temperature and Pressure. *Ind. Eng. Chem. Res.* **1992**, *31* (8), 2033–2039.

(52) Hsieh, C. M.; Lin, S. T.; Vrabec, J. Considering the Dispersive Interactions in the COSMO-SAC Model for More Accurate Predictions of Fluid Phase Behavior. *Fluid Phase Equilib.* **2014**, *367*, 109–116.

(53) Stryjek, R.; Vera, J. H. PRSV: An Improved Peng—Robinson Equation of State for Pure Compounds and Mixtures. *Can. J. Chem. Eng.* **1986**, *64* (2), 323–333.

(54) Proust, P.; Meyer, E.; Vera, J. H. Calculation of Pure Compound Saturated Enthalpies

and Saturated Volumes with the PRSV Equation of State. Revised k1 Parameters for Alkanes. *Can. J. Chem. Eng.* **1993**, *71* (2), 292–298.

(55) Proust, P.; Vera, J. H. PRSV : The Stryjek-Vera Modification of the Peng-Robinson Equation of State. Parameters for Other Pure Compounds of Industrial Interest. *Can. J. Chem. Eng.* **1989**, *67*, 170–173.

(56) Nelder, J. A.; Mead, R. A Simplex Method for Function Minimization. *Comput. J.* **1965**, *7* (4), 308–313.

(57) Miroshnichenko, S.; Vrabec, J. Excess Properties of Non-Ideal Binary Mixtures Containing Water, Methanol and Ethanol by Molecular Simulation. *J. Mol. Liq.* **2015**, *212*, 90–95.

(58) Smith, J. M.; Van Ness, H. C.; Abbott, M. M. *Introduction to Chemical Engineering Thermodynamics*, 5th ed.; , McGraw-Hill: New York, 1996.

(59) Hsieh, M.-K.; Lin, S.-T. Effect of Mixing Rule Boundary Conditions on High Pressure (Liquid+liquid) Equilibrium Prediction. *J. Chem. Thermodyn.* **2012**, *47*, 33–41.

(60) Stubbs, J. M.; Siepmann, J. I. Aggregation in Dilute Solutions of 1-Hexanol in N-Hexane: A Monte Carlo Simulation Study. *J. Phys. Chem. B* **2002**, *106*, 3968–3978.

(61) Egloff, G. *Physical Constants of Hydrocarbons*; Reinhold Publishing: New York, 1939.

(62) Francis, A. Pressure-Temperature-Liquid Density Relations of Pure Hydrocarbons. *Ind. Eng. Chem.* **1957**, *49* (10), 1779–1786.

(63) William Prengle Jr., H.; Felton, E. G.; Pike Jr., M. A. Thermodynamics of Solutions--

Volume Change on Mixing for Four Systems. *J. Chem. Eng. Data* **1967**, *12* (2), 193–196.

(64) Campbell, A. N.; Chatterjee, R. M. Orthobaric Data of Certain Pure Liquids in the Neighborhood of the Critical Point. *Can. J. Chem.* **1968**, *46*, 575–581.

(65) Friend, J. N.; Hargreaves, W. D. VII. Viscosities at the Boiling Point of Some Primary Amines, Cyclohexane and Some of Its Derivatives. *London, Edinburgh, Dublin Philos. Mag. J. Sci.* **1944**, *35* (240), 57–64.

(66) Timmermans, J. *Physico-Chemical Constants of Pure Organic Substances, Vol II*; , Elsevier: New York, 1965.

(67) Hugill, J. A.; McGlashan, M. L. The Vapour Pressure from 451 K to the Critical Temperature, and the Critical Temperature and Critical Pressure, of Cyclohexane. *J. Chem. Thermodyn.* **1978**, *10* (1), 95–100.

(68) Kerns, W.; Anthony, R.; Eubank, P. In: AIChE Symposium Series. **1974**, *70* (140), 14–21.

(69) Bender, P.; Furukawa, G. T.; Hyndman, J. R. Vapor Pressure of Benzene above 100 °C. *Ind. Eng. Chem.* **1952**, *44* (2), 387–390.

(70) Ambrose, D.; Ghiassee, N. B. Vapour Pressures and Critical Temperatures and Critical Pressures of C5 and C6 Cyclic Alcohols and Ketones. *J. Chem. Thermodyn.* **1987**, *19* (9), 903–909.

(71) Boublik, T.; Fried, V.; Hala, E. *The Vapor Pressures of Pure Substances*; Elsevier: New York, 1973.

(72) Daubert, T. E.; Jalowka, J. W.; Goren, V. Vapor Pressure of 22 Pure Industrial

Chemicals. *AIChE Symp. Ser.* **1987**, *83* (256), 128–156.

(73) Novak, J.; Natouš, J.; Pick, J. Gleichgewicht Flüssigkeit-Dampf XXIV. Gleichgewicht Flüssigkeit-Dampf Im System Cyclohexylamin-Cyclohexanol-Anilin. *Collect. Czechoslov. Chem. Commun.* **1960**, *25* (9), 2405–2413.

(74) Carswell, T. S.; Morril, H. L. Cyclohexylamine and Dicyclohexylamine: Properties and Uses. *Ind. Eng. Chem.* **1937**, *29* (11), 1247–1251.

(75) Ramsay, W.; Young, S. LXVIII.—A Method for Obtaining Constant Temperatures. *J. Chem. Soc. Trans.* **1885**, *47*, 640–657.

(76) Garrick, F. J.; Gray, R. W. The Vapour Pressures of Diphenyl and of Aniline. *Trans. Faraday Soc.* **1927**, *23*, 560–563.

(77) Kozicki, W.; Sage, B. H. Latent Heat of Vaporization of Cyclohexane. *Chem. Eng. Sci.* **1961**, *15* (3–4), 270–275.

(78) Young, S. The Internal Heat of Vaporization. *J. R. Dublin Soc.* **1910**, *12*, 374–443.

(79) Hwang, C.-A.; Elkabule, A. .; Whitman, D. .; Miller, R. . Excess Molar Enthalpies of (Benzene + Cyclohexane + N-Hexane). *J. Chem. Thermodyn.* **1987**, *19* (10), 1031–1036.

(80) Weeks, I. A.; Benson, G. C. Determination of the Excess Volume of Cyclohexane + Benzene by Means of a Magnetic Float Densimeter. *J. Chem. Thermodyn.* **1973**, *5* (1), 107–117.

(81) Kirss, H.; Kuus, M.; Siimer, E.; Kudryavtseva, L. Excess Enthalpies for the Ternary Mixtures Phenol-1-Hexanol-N-Heptane and Phenol-Cyclohexanol-N-Heptane, and

Their Constituent Binaries at 318.15 K. *Thermochim. Acta* **1995**, *265*, 45.

(82) Grenner, A.; Klauck, M.; Kramer, M.; Schmelzer, J. Activity Coefficients at Infinite Dilution of Cylcohexylamine + Octane, Toluene, Ethylbenzene, or Aniline and Excess Molar Volumes in Binary Mixtures of Cyclohexylamine + Heptane, Octane, Nonane, Decane, Undecane, Aniline, or Water. *J. Chem. Eng. Data* **2006**, *51* (1), 176.

Acknowledgments

We gratefully acknowledge the help of Denis Šarić, Andreas Köster and Tatjana Janzen during the simulation runs. The simulations were carried out on the Cray XC40 (Hazel Hen) computer at the High Performance Computing Center Stuttgart (HLRS) and on the the OCuLUS cluster of the Paderborn Center for Parallel Computing (PC^2). C.-M. Hsieh also acknowledges support from the Ministry of Science and Technology of Taiwan (Grants MOST 105-2221-E-008-106).

Table of Content

TOC Graphic